PCCP

View Online
Dynamic Article Links

Cite this: *Phys. Chem. Chem. Phys.*, 2011, **13**, 4500–4506

www.rsc.org/pccp

PAPER

Bi-analyte single molecule SERS technique with simultaneous spatial resolution†

Pablo G. Etchegoin,*[a] Eric C. Le Ru[a] and A. Fainstein[b]

Received 31st October 2010, Accepted 22nd December 2010
DOI: 10.1039/c0cp02335c

The simultaneous combination on CCD detectors of both spectral and spatial information is used in the framework of the single molecule (SM) bi-analyte Surface-Enhanced Raman Scattering (SERS) technique, to provide a new level of understanding on the origins of SM-spectra, as well as reveal the advantages and limitations of the statistical identification of SM-events. A new and deeper interpretation of the roots of the inhomogeneous broadening of single molecule Raman peaks can be uncovered, as well as the origin of Surface-Enhanced Fluorescence (SEF) emission by single molecules. In this manner, subtler aspects of SM-SERS spectroscopy can be revealed by the additional presence of spatial information on the localization of single molecules producing the signal. The spatial information is normally lost through the standard binning of CCD cameras for spectroscopy, which only emphasizes the spectral dimension of the problem. This novel extension of the bi-analyte SM-SERS method should contribute to the furtherance of the technique, and several of its fundamental aspects are discussed in detail.

I. General overview

The field of single molecule (SM) Surface-Enhanced Raman Scattering (SERS)[1,2] is now in a mature state to allow studies beyond the mere demonstration of SM-sensitivity[3–9] (which has been much debated for roughly a decade).[10] With variations around Tip-Enhanced Raman Scattering (TERS),[11,12] Langmuir–Blodgett films[13] and bi-analyte techniques,[14–17] it has been possible to extend our understanding of single molecule detection with SERS in various possible directions. In this paper, we shall concentrate exclusively on perfecting the technique of bi-analyte SM-SERS, which has now been extended to different levels of sophistication (including isotopic editing of dyes).[16–18] The technique has been already used not only to provide a sound statistical proof of SM-sensitivity[14] but also to: (*i*) resolve the inhomogeneous broadening of single molecule Raman peaks[17,19]; (*ii*) demonstrate natural isotopic substitutions in single molecule spectra[20]; (*iii*) work in combination with Langmuir–Blodgett films[13]; (*iv*) demonstrate single-molecule vibrational pumping[21] and photobleaching[22]; quantify SM-SERS enhancement factors of pre-resonant[23] and non-resonant[24] molecules; and (*v*) observe single molecule electrochemistry.[6,25]

Herewith, we add a new layer of understanding into the origin and use of the bi-analyte SM-SERS technique, namely: the possibility of combining simultaneously both spectral and spatial information together with single molecule detection. In the process of doing this, we shall show: (*i*) the origin of the inhomogeneous broadening of Raman peaks,[17,19] but from a more fundamental point of view that combines spatial information on the localization of the molecules, (*ii*) an extension that demonstrates the roots (and ultimately the limits) of the statistical determination of SM-SERS events in the bi-analyte technique; and (*iii*) the phenomenon of Surface-Enhanced Fluorescence (SEF)[26] in conditions where it can be traced back to individual single molecules emitting the SERS background. Hence, the simultaneous combination of spectral and spatial information results in a deeper understanding of the subtler aspects of SM-SERS detection with the bi-analyte technique.[14]

It is probably worth emphasising at this stage that there is a whole family of microscopy techniques that have been developed in last few years (and decades) that make emphasis on super-resolution,[27,28] while other microscopic (imaging) techniques have been directly applied to SM-SERS problems.[3,29,30] In the cases that are directly relevant for this paper[3,30] the emphasis has been put in full imaging; *i.e.* a situation where part of the spectral information is lost by filtering in a certain spectral window. In Aroca's work, for example, the spectra is filtered in a certain range and then it is imaged on the CCD. The technique applied here, however, is more related to what is done normally in cytometry,[31] where a mixture of spatial and spectral information is used at the same time. The spatial component is not

[a] *The MacDiarmid Institute for Advanced Materials and Nanotechnology, School of Chemical and Physical Sciences, Victoria University of Wellington, PO Box 600, Wellington, New Zealand. E-mail: Pablo.Etchegoin@vuw.ac.nz*
[b] *Centro Atómico Bariloche and Instituto Balseiro, Comisión Nacional de Energía Atómica and Universidad Nacional de Cuyo, (8400) San Carlos de Bariloche, Río Negro, Argentina*
† Electronic supplementary information (ESI) available. See DOI: 10.1039/c0cp02335c

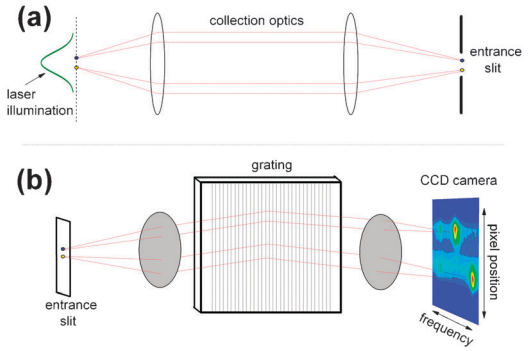

Fig. 1 Schematic representation of dual frequency-position determination of SM-SERS signals.[32] (a) The illumination envelop of the laser (typically Gaussian) produces single molecule Raman signals at different hot-spots. These signals can be of the same or different type of molecules in the bi-analyte technique.[14] The spot on the sample is imaged onto the entrance slit of the spectrometer with a magnification defined by the collecting optics (a factor of 56 in our system).[23] (b) The spectral content of the image at the entrance slit is resolved on the CCD in the direction perpendicular to the grooves of the grating. In the direction along the grooves, however, the spectrometer works as a normal imaging device and can resolve two point sources in one direction (with some limitations explained in the Supplementary Information to the paper).[33] This results, accordingly, in a mixed frequency-position image on the CCD (widely used in spatially-resolved fluorescence spectroscopy).[31] The combination of this capability with the bi-analyte SERS technique is exploited in this paper explicitly. In the example given here two different molecules (resolved in frequency) are distinguished in the vertical direction (resolved in space) simultaneously.

particularly high resolution, but it comes with the advantage of being able to distinguish spectral features.

Fig. 1 shows the basic concept of the experiment. Two point-like sources (which will represent single hot-spots later) are illuminated by a laser at the object plane, and subsequently imaged onto the entrance slit of the spectrometer (with a given magnification) by the collecting optics of the experiment (Fig. 1(a)). Once inside the spectrometer (Fig. 1(b)) the grating separates the image according to its spectral content, but some degree of spatial information can also be retained in the direction parallel to the grating's grooves. This defines then a *spatial* and a *spectral* direction on the CCD plane. In the spatial direction, the instrument behaves essentially as a standard imaging microscope subject to the natural limitations imposed by the diffraction limit and residual aberrations. As mentioned before, the idea of combining spatial and spectral information simultaneously is certainly not new,[32] but has rather been used extensively in the field of fluorescence spectroscopy (in particular for applications in cytometry).[31] However, it has never been used to best of our knowledge in the field of SM-SERS and it provides, as we shall show later, a much deeper understanding into the foundations of the statistical analysis and the single molecule sensitivity of the technique.

II. Bi-analyte SERS with spatial resolution

A General aspects

The bi-analyte SM-SERS technique[14] is a contrast method, where the statistical fluctuations of the signal of one molecule are analyzed in the background of the statistics of a "partner" molecule; which serves both as a reference and analyte in its own right. The statistical interpretation has been now extensively studied in the literature.[34] For our present purposes, we take the case of SM-SERS on dry substrates of Lee & Meisel Ag (citrate reduced) colloids[35] deposited on poly-L-lysine covered Si substrates as an archetypical example (widely used in the literature). The experimental conditions for sample preparation in this paper are identical to those reported elsewhere.[19]

For most of the examples shown in this paper we chose Nile Blue (NB) and Rhodamine 6G (RH6G) as bi-analyte partners (5 nM concentration each). Despite the fact that NB has a larger Raman differential cross section than RH6G at the excitation wavelength used here (633 nm), they constitute two convenient partners that have been already used in SM-studies in the past.[23] More importantly, they provide two very convenient fingerprint modes at 590 cm^{-1} (NB) and 612 cm^{-1} (RH6G) that are well separated from each other on the CCD images even at moderate resolution. This is an advantage over isotopic probes[16–18] which tend to have spectral fingerprints that are much closer, and present more of a challenge to distinguish at low resolution. An example of isotopic probes will be shown in the last section, after we study the more convenient bi-analyte probes combination of NB/RH6G. We use a LabRam spectrometer (600 l mm^{-1} grating) equipped with an Olympus BX41 microscope and a $\times$ 100 (NA = 0.9) objective for our experiments. The integration time was fixed to 1 s to take CCD images in different parts of the sample (as in a spatial mapping mode) with 3 mW incident power (633 nm). CCD images were restricted to the region 550–660 cm^{-1} in frequency, and to 40 pixels in the spatial direction, respectively. This is because taking full images requires a large readout time and the sample has a chance to change during acquisition if the full CCD image (1024 $\times$ 256 pixels) is read. The next subsections summarize the most important results that can be gained by the addition of spatial resolution in SM-SERS. We shall show, in addition, an example for isotopically edited bi-analyte partners (methyl-ester rhodamines (RH6M) synthesized in ref. 16) at the end.

B Single molecule events

Fig. 2(a–c) show the first important concept in these experiments: the detection of three different single molecule NB events at different positions on the spatial axis of the CCD. In fact, we can "project" the images on the spatial axis (*i.e.* by summing pixels along the frequency axis) and observe different SM-events, as shown in Fig. 2(d) for four different NB SM-SERS events. We also show in Fig. 2(d) the intensity profile one gets for the 520 cm^{-1} Raman mode of Si on a clean wafer under the same experimental conditions, projected again onto the spatial axis dimension. There are issues of aberrations in these images introduced by the natural astigmatism of the machine in the direction parallel to the grooves of the grating.[36] For example the typical width of SM-events in Fig. 2(d) along the spatial axis comes from the so-called astigmatic point spread function of the instrument. This is a well known phenomenon[31] and interesting in its own right, but it is

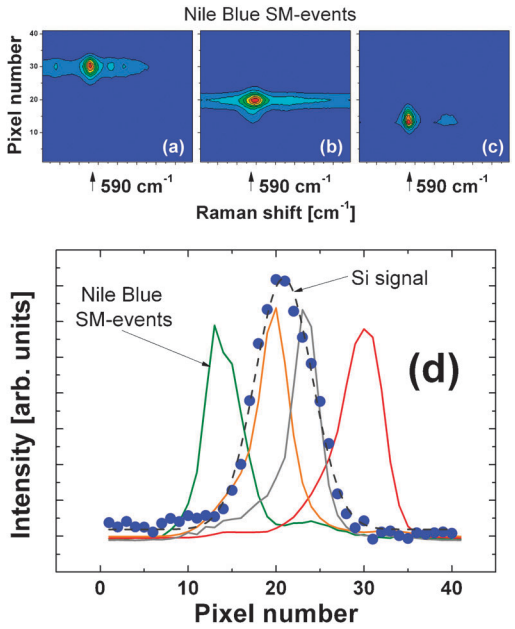

Fig. 2 (a-c) Examples of SM-SERS events from Nile Blue at different positions on the spatial axis of the CCD. These are events where RH6G was not present in the spectra. In (d) we show four examples of this type of events with signals that are integrated in the frequency dimension of the CCD. We also show the illumination profile of the Raman signal on a Si substrate (520 cm^{-1}) obtained under the same experimental conditions. Single molecule events can be detected all the way into the tails of the illumination envelope, due to both the effect of large enhancements at hot-spots and the perturbation of the illumination envelope by the presence of clusters (see the Supplementary Information for more details). The SM-events have been rescaled to similar intensities for visualization purposes only, but they can occur with different intensities depending on the specific hot-spot where the molecule is; with some events on the "wings" of the beam being sometimes more intense than events in the center.

somewhat collateral to our purposes here. A much lengthier discussion on the meaning of these profiles is given in the Supplementary Information (SI) to this paper for the interested reader. As far as the discussion here is concerned, we content ourselves with the fact that SM-SERS signals can, effectively be detected at different spatial positions on the CCD. Note, in addition, that the data in Fig. 2(d) suggests that SM events can be detected all the way through the illumination envelope (including the "wings") produced on a flat surface like Si. This is, in fact, a unique characteristic of the SM-SERS problem and the presence of hot-spots,[37] which can reach enhancement factors up to $\sim 10^{10}$ in some cases[23] and make visible SM-SERS signals even if they are on the periphery of the illumination region. But it is also a consequence of the spread in the illumination (and its effect on the tail of the beam) caused by the presence of metallic clusters on the sample. The distance over which two SM-SERS events can be spatially resolved is again the matter of a lengthier discussion in the Supplementary Information to the paper. For our present discussion here, it suffices to say that molecules of the same type can be distinguished as separate peaks on the spatial axis for separations that are in the range 800 nm–5 μm; *i.e.* well above the diffraction limit. Accordingly, there is no claim here of super-resolution or similar assertions,[3] but only the fact that we can resolve spatially (with some limitations) the presence of more than one peak. This characteristic is the only experimental fact that we need to carry over, as far as the rest of the analysis in the paper is concerned. The spatial separation comes, in addition, from a direct visual inspection of the images; *i.e.* it does not rely on extensive data analysis or processing algorithm, as it is required in other cases.[3]

It is also important to reemphasize that we can only achieve spatial resolution in *one* direction, and all the examples shown here are ones in which that condition was obviously fulfilled. But there are many situations where this is not the case, and this is a natural price to pay for the sake of obtaining simultaneously spatial and spectral information. In many cases, for example, signals of NB and RH6G at the same pixel positions (in the spatial direction) are observed. These signals can be produced either because they come from the same hot-spot (and they are spectrally resolved), or because they come from two different hot spots aligned in the direction where the spectral dispersion is done. We cannot decide the real origin in this framework.

C Two and three molecule events

The ability to resolve a SM-SERS event spatially in one direction opens up now the more interesting possibility of observing more than one molecule of the same type. To continue with the analysis started in Fig. 2, we concentrate again on cases where RH6G is absent and only NB signals are observed, but exactly the same phenomenology exists for the opposite case. Fig. 3 shows several examples where two clear NB peaks can be observed; with different intensities, different spatial localizations, and slightly different frequencies.[17,19] These events are obviously rarer than the single molecule ones (of the type shown on Fig. 2), but they do appear at the chosen analyte concentration. Fig. 3(a–f) show six different examples. Note that, as far as the conventional bi-analyte SERS method is concerned, all these events would be categorized as "pure" spectra, since the different contributions will be lost in the binning along the spatial dimension. As an example, Fig. 3(g) shows a more detailed analysis of the image in Fig. 3(b). We note here that if the signal at pixel numbers 13 and 33 are plotted independently, we can identify the SM-spectra of the two hot-spots in the image with slightly different frequencies for the NB peak. We also note that the frequency difference is small enough *not* to be apparent in the average spectrum in Fig. 3(g) (summed over the spatial dimension). From the result of the average spectrum we could not have reliably concluded that the peak had contributions from more than one molecule. This small frequency difference could have been resolved with higher resolution in the spectral dimension (as done in ref. 19). But here we are, in a way, recovering a result that we would have obtained at higher resolution from the average spectrum by using the additional degree of freedom of the spatial dimension. One aspect does not replace the other, but they are rather complementary and represent two alternative ways of looking at the same problem. In our case here, we are compensating "lack of spectral resolution" in the frequency domain to resolve the inhomogeneous broadening with

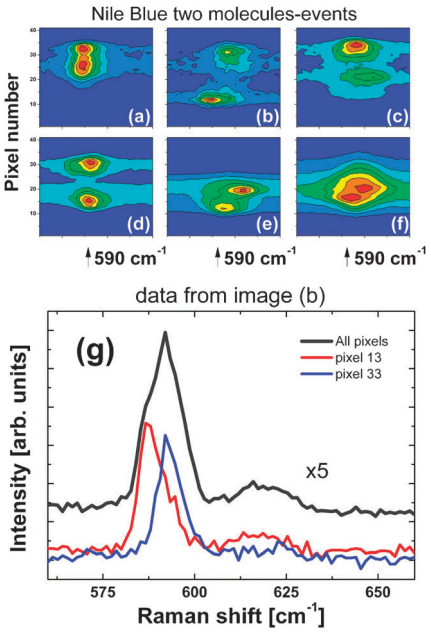

Fig. 3 (a-f) Six different examples of NB signals (without RH6G) in which *two* molecules can be distinguished in the spatial dimension. Note that peaks are not only spatially resolved but also appear at slightly different frequencies. In (g) we show a more detailed analysis of the image in (b). If the image is sliced along pixel numbers 13 and 33, the two different peaks at different frequencies can be resolved. Note that we could not have resolved them from the average spectrum binned in the spatial direction (also shown in (g)). The two peaks could have been resolved with higher resolution, but we are basically recovering the same information by the addition of the spatial dimension. See the text for further details.

"spatial information" to arrive at the same conclusion; *i.e.* that the spectrum had contributions from more than one molecule. In general, however, most experiments will be carried out at relatively low resolution. One inconvenience of higher resolution setups besides the limited spectral range is the reduced throughput and lower light count per pixel, with the concomitant smaller signal-to-noise ratio.

There is a subtlety though here that is worth keeping in mind, even when we will generally ignore its effects. It is interesting however to understand the details of it, to appreciate how the different aspects of spatial and spectral resolution are intimately intertwined with both the physics of the sample and the measurement device (spectrometer). It is only partially true that there is no spatial information at all in the spectral dimension. In fact, the frequency of a peak can be modified slightly by the position of the spot at the entrance slit (in the dispersion direction) with respect to the optical axis. This is one of the possible origins of the inhomogeneous broadening of SM-SERS lines, which has been thoroughly studied before.[19] In that sense, peaks that are detected as "spectrally separated" could be *either* due to molecules in slightly different environments (a property of the sample), *or* to a spatial separation along the dispersion direction (a property of the measurement). Accordingly, the information we would regain by a higher resolution measurement is –strictly speaking– not the same that the one we would obtain from spatial information. For example, two molecules that have exactly the same frequency but are spatially at different hot-spots cannot be resolved even if high resolution measurements are carried out. But they will appear as two different peaks in the spatial direction in many cases. On the contrary, two molecules that appear at slightly different frequencies might not be resolvable in the spatial direction but would appear as two definite peaks in a higher resolution measurement; if the frequency difference is physical and has its origin in slightly different situations for both molecules on the sample. Hence, the spatial information adds a unique type of insight into the origin of the SM-SERS signals that is not (necessarily) equivalent to the information gained from the spectral dimension, at any degree of resolution. We will not consider this for the rest of the discussion, but it is worth knowing that the method used here can reveal aspects of SM-SERS that would not be evident if only data in the spectral domain is analyzed (at any degree of resolution).

We believe these examples provide a deeper understanding of the fundamental origin of the inhomogeneous broadening of SM-SERS spectra, with the new information here being complementary (in the sense explained above, *vide supra*) to the one obtained by resolving the individual molecules in the spectral dimension. For example, we can conclude more confidently in this case that the signals come from *different* hot-spots; an aspect that is actually lost when the spatial information of the CCD is binned to provide the spectral axis only. The results also show that, despite being a minority in the statistics, many multiple molecule events can be avoided by decreasing the lateral extent of the scattering volume (which in our system can be achieved by closing the confocal pinhole).[23] This has been tried before,[19] but our new results show the microscopic origin and rationale of the method: a smaller scattering volume avoids signals from multiple hot-spots that are spatially resolved but contribute to the total signal otherwise. Last, but not least, on statistics of hundreds of images it is indeed possible to find events with *three* molecules of the same type; an example of which is shown in Fig. 4. While these events are certainly a rare minority in the statistics, they do present themselves as expected. Fig. 4 shows again an example in which the contributions from the three molecules could not have been disentangled from the total (binned) signal in the spatial dimension of the CCD.

D Mixed events

Besides the single-molecule events, and multiple molecule events of the same type of analyte, there are of course *mixed events* in which both bi-analyte partners appear. These events are automatically discarded in the standard implementation of the bi-analyte SERS technique, but it is interesting to look at them in the light of the spectral-spatial decomposition of the signal. Fig. 5 shows two examples of the latter. As before, we show cases in which there is more information than the mere observation of the two bi-analyte parteners, *i.e.* we show cases which are a "minority" in the statistics but where the addition of spatial resolution adds an interesting new detail. Fig. 5(a), for example, shows a mixed event case where we can distinguish more than two molecules. The RH6G and NB signals are not exactly at the same pixel position (suggesting that they come from two different hot-spots) and if we plot the intensity by

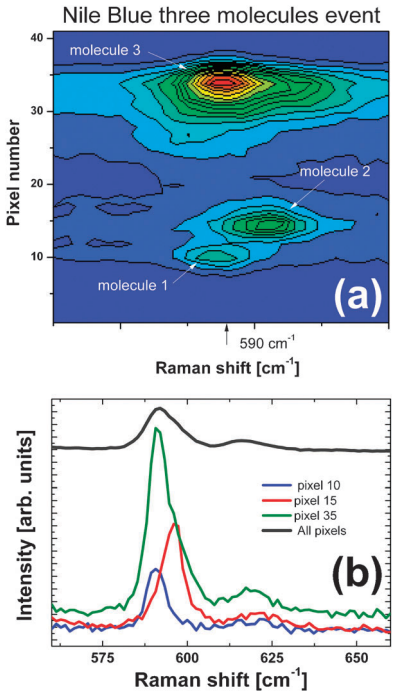

Fig. 4 An event with three molecules of the same type (NB) and no RH6G. As in Fig. 3, the molecules could not have been resolved from the average spectrum, but they appear clearly resolved in the spatial dimension with different intensities and frequencies. These events are a *minority* in the statistics, but they do occur over hundreds of images at the chosen analyte concentration.

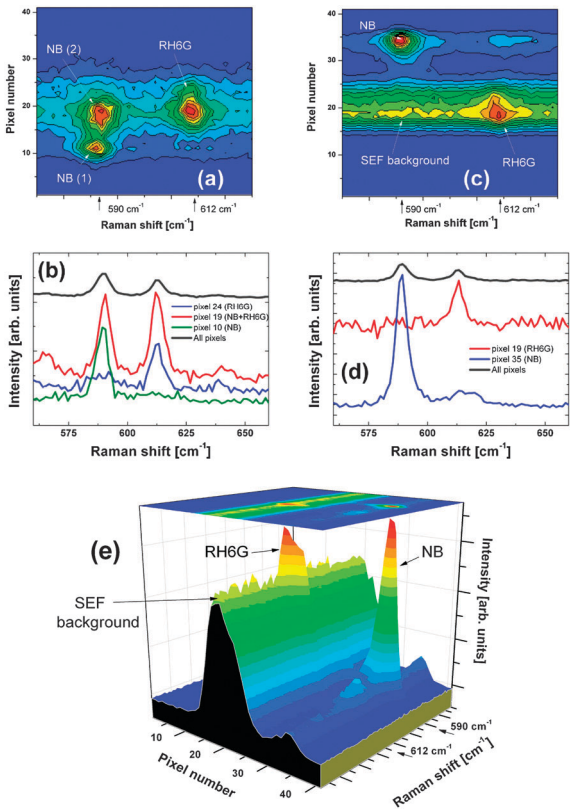

Fig. 5 Mixed events of NB + RH6G showing a few details that can be only resolved with the aid of spatial resolution. In (a) we show a mixed event which contains at least three different molecules/hot-spots: two with signals of NB and one with RH6G. The RH6G signal is slightly displaced from the closest NB one in the spatial direction. If the image is sliced along different pixels (as shown in (b)) we can distinguish spectra that look like pure NB, NB + RH6G, and pure RH6G, respectively. This would represent then a three-molecule mixed event. In (c-e) we show another interesting case of a mixed NB + RH6G in which one of the molecules (RH6G) is emitting a SEF background.[26,38] The average spectrum in (d) contains the two Raman peaks of NB and RH6G and the background. The slicing of the image in the spatial direction in fact reveals a background-free NB peak, and a RH6G Raman peak on top of the background. This is shown more explicitly in (e) showing the 3D plot of the same image as (c). It is also possible to find events where the background comes entirely from the NB molecule. These experiments show that the backgrounds can be traced back to individual molecules.

slicing the image for different pixels (as it is done in Fig. 5(b)) we can resolve spectra that look like pure NB, mixed NB + RH6G, and pure RH6G, respectively. We can claim therefore that this is a mixed event with contributions from at least three molecules/hot-spots: two NBs and one RH6G.

Fig. 5(c–d) show another interesting aspect that we only have access to with the addition of spatial resolution. A NB + RH6G mixed event is shown in Fig. 5(c); the signals are not only spatially separated but also we note that one of the molecules (RH6G) is emitting a background (seen as a horizontal stripe) while the other is not. If we had observed the average spectrum only, by binning the pixels into the spatial dimension, we would have observed a mixed event with a background without any further information on the actual origin of the background itself. The spatial separation of the image not only allows us to identify the origin as two separate NB and RH6G Raman contributions, but also allows us to unequivocally identify the background with one of the molecules only. The fact that the background is linked to one of the molecules is actually better visualized if we plot the intensity map in a 3D representation, as shown in Fig. 5(e).

The origin of SERS backgrounds has been extensively debated in the literature.[39,40] Our preferred interpretation is based on the phenomenon of Surface-Enhanced Fluorescence (SEF) when it results in a spectral modification of the emission.[26,38] The SEF background is, in fact, very sensitive to the exact distance of the molecule from the surface; with a fraction of a nanometre making a substantial difference to the ratio of radiative to total emission.[38] It is not the purpose here to go into any depth into the details of the origin of the background, but rather to point out the experimental fact that we can trace it back to an individual molecule. We have observed both NB and RH6G individual events with or without background, which strongly suggests that it is, indeed, related to the specific situation of that particular molecule at a given hot-spot. A similar phenomenon of individual molecules emitting a SEF background has also been observed for the isotopically edited bi-analyte pair shown in the next sub-section.

E Isotopically edited molecules

Isotopically edited dyes for SERS are becoming of age now,[41] and have provided so far the cleanest examples of bi-analyte SERS partners.[16–18] All the results obtained here for the

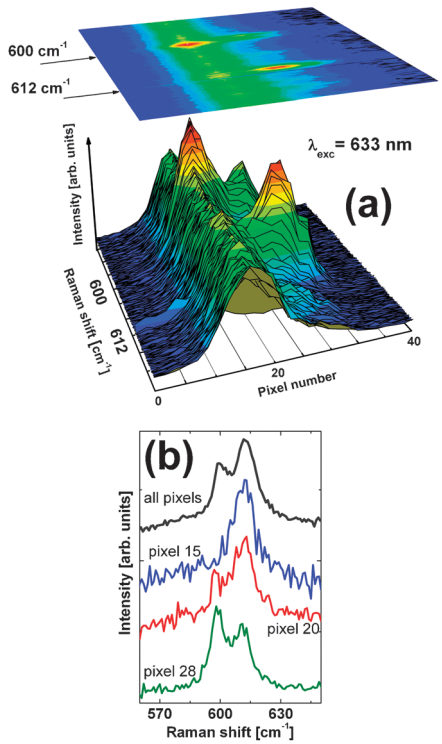

Fig. 6 An example of bi-analyte SERS frequency-position image for the isotopic pair RH6M and d_4-RH6M.[16] These are the methyl ester versions of the same dyes used in ref. 17, and have been fully characterized as bi-analyte SERS partners in ref. 16. The image is taken in the region of the fingerprint modes of RH6M at 612 cm^{-1} and d_4-RH6M at 600 cm^{-1}, respectively. The image in (a) corresponds to a mixed event in which signals of both dyes can be seen. There is a background emission clearly associated with the d_4-RH6M peak that represents Surface-Enhanced-Fluorescence (SEF)[2] of that particular molecule. The background is not present for RH6M. In (b) we show the full spectrum we would have obtained if all the bins of the CCD are summed in the spatial dimension (normal bi-analyte method). By spatially resolving the spectra along different pixels, however, we can see the different contributions that the two molecules make to the total spectra. See the text for further details.

NB/RH6G partners can also be obtained for isotopically substituted dyes. Fig. 6 shows a specific example for the isotopically substituted methyl ester versions of rhodamine (synthesized in ref. 16), where several of the aspects discussed before are present. The figure shows, for example, a mixed event with two spatially resolved signals for RH6M and d_4-RH6M at 612 and 600 cm^{-1}, respectively, with one of the molecules (d_4-RH6M) emitting a SEF background. However, the reason why we used the NB/RH6G system instead for the vast majority of results is because the clearest fingerprint peaks from isotopic substitution in RH6M and d_4-RH6M have some degree of spectral overlap for the resolution used here and, therefore, it is sometimes difficult to disentangle the natural "wobbling" of the frequencies[17] with the presence of an overlap. A much clearer example of individual frequencies moving in individual or mixed events is obtained if we look at bi-analyte partners with a larger frequency separation between fingerprint modes, and that is more easily achieved with the pair NB/RH6G. But except for that technicality, the same conclusions can be obtained in isotopically substituted bi-analyte partners.

III. Conclusions

The addition of spatial information for the bi-analyte SERS method adds a new dimension into the statistical interpretation of the details of the technique. The observation of a few molecules of the same or different type that are spatially resolved and contribute to both the inhomogeneous broadening and the statistics of mixed events can be manifestly put into evidence. Moreover, the spatial information adds the observation of SERS backgrounds that can be truly tracked down to individual molecules/hot-spots and can, therefore, be attributed to a single molecule property. We believe the presence of SEF backgrounds is related to the exact position of the molecule with respect to the surface, which can make a substantial difference for the ratio of radiative to total emission (as studied in more detail elsewhere).[38] Moreover, these experiments provide a complementary demonstration of the origin of the inhomogeneous broadening of single molecule Raman peaks, in which the information that is lost by spectral resolution[19] can be sometimes regained by spatial discrimination. The technique can put in evidence contributions from more than one molecule in the spatial direction in situations where this information could not have been gained by arbitrary high spectral resolution. The method, therefore, intertwines in several ways the different aspects of the fundamental origin of the inhomogeneous broadening of Raman peaks with the physics of the detection system itself (spectrometer). Overall, we believe our contribution here is another demonstration of the type of studies that SM-SERS is capable of now, by revealing subtler details of the spectroscopy of single molecules beyond the mere demonstration of SM-sensitivity.

Acknowledgements

P.G.E. and E.C.L.R. are indebted to the Royal Society of New Zealand for partial financial support under a Marsden Grant. Useful exchanges with J. Lerner (LightForm, Inc.) are gratefully acknowledged.

References

1 R. F. Aroca, *Surface-Enhanced Vibrational Spectroscopy*, John Wiley & Sons, Chichester, 2006.
2 E. C. Le Ru and P. G. Etchegoin, *Principles of Surface Enhanced Raman Spectroscopy and Related Plasmonic Effects*, Elsevier, Amsterdam, 2009.
3 S. M. Stranahan and K. A. Willets, *Nano Lett.*, 2010, **10**, 3777.
4 G. Haran, *Acc. Chem. Res.*, 2010, **43**, 1135.
5 W. H. Park and Z. H. Kim, *Nano Lett.*, 2010, **10**, 4040.
6 D. P. dos Santos, G. F. Andrade, M. L. A. Temperini and A. G. Brolo, *J. Phys. Chem. C*, 2009, **113**, 17737.
7 G. Haran, *Isr. J. Chem.*, 2004, **44**, 385.
8 D. R. Ward, N. J. Halas, J. W. Ciszek, J. M. Tour, Y. Wu, P. Nordlander and D. Natelson, *Nano Lett.*, 2008, **8**, 919.
9 N. P. W. Pieczonka and R. F. Aroca, *Chem. Soc. Rev.*, 2008, **37**, 946.
10 P. G. Etchegoin and E. C. Le Ru, *Phys. Chem. Chem. Phys.*, 2008, **10**, 6079.
11 K. F. Domke and B. Pettinger, *ChemPhysChem*, 2010, **11**, 1365.
12 B. Pettinger, *Mol. Phys.*, 2010, **108**, 2039.
13 P. J. G. Goulet and R. F. Aroca, *Anal. Chem.*, 2007, **79**, 2728.
14 E. C. Le Ru, M. Meyer and P. G. Etchegoin, *J. Phys. Chem. B*, 2006, **110**, 1944.
15 Y. Sawai, B. Takimoto, H. Nabika, K. Ajito and K. Murakoshi, *J. Am. Chem. Soc.*, 2007, **129**, 1658.

16 E. Blackie, E. C. Le Ru, M. Meyer, M. Timmer, B. Burkett, P. Northcote and P. G. Etchegoin, *Phys. Chem. Chem. Phys.*, 2008, **10**, 4069.
17 J. A. Dieringer, R. B. L. II, K. A. Scheidt and R. P. V. Duyne, *J. Am. Chem. Soc.*, 2007, **129**, 16249.
18 D. M. Zhang, Y. Xie, S. K. Deb, V. J. Davisson and D. Ben-Amotz, *Anal. Chem.*, 2005, **77**, 3563.
19 P. G. Etchegoin and E. C. Le Ru, *Anal. Chem.*, 2010, **82**, 2888.
20 P. G. Etchegoin, E. C. Le Ru and M. Meyer, *J. Am. Chem. Soc.*, 2009, **131**, 2713.
21 C. M. Galloway, E. C. Le Ru and P. G. Etchegoin, *Phys. Chem. Chem. Phys.*, 2009, **11**, 7372.
22 P. G. Etchegoin, P. D. Lacharmoise and E. C. Le Ru, *Anal. Chem.*, 2009, **81**, 682.
23 E. C. Le Ru, E. Blackie, M. Meyer and P. G. Etchegoin, *J. Phys. Chem. C*, 2007, **111**, 13794.
24 E. J. Blackie, E. C. Le Ru and P. G. Etchegoin, *J. Am. Chem. Soc.*, 2009, **131**, 14466.
25 E. Cortés, P. G. Etchegoin, E. C. Le Ru, A. Fainstein, M. Vela and R. Salvarezza, *J. Am. Chem. Soc.*, 2010, **132**, 18034.
26 E. C. Le Ru, P. G. Etchegoin, J. Grand, N. Felidj, J. Aubard and G. Levi, *J. Phys. Chem. C*, 2007, **111**, 16076.
27 S. W. Hell and M. Kroug, *Appl. Phys. B: Lasers Opt.*, 1995, **60**, 495.
28 S. Bretschneider, C. Eggeling and S. W. Hell, *Phys. Rev. Lett.*, 2007, **98**, 218103.
29 S. Schlucker, *Surface Enhanced Raman Spectroscopy: Analytical, Biophysical and Life Science Applications*, Willey-VCH, Weinheim, 2010.
30 C. J. L. Constantino, T. Lemma, P. A. Antunes and R. Aroca, *Anal. Chem.*, 2001, **73**, 3674.
31 J. M. Lerner, *Cytometry, Part A*, 2006, **69A**, 712.
32 E. C. Le Ru and P. G. Etchegoin, *Chem. Phys. Lett.*, 2004, **396**, 393.
33 M. Born and E. Wolf, *Principles of Optics*, Pergamon Press Ltd., Oxford, 6th-edn, 1980.
34 P. G. Etchegoin, M. Meyer, E. Blackie and E. C. Le Ru, *Anal. Chem.*, 2007, **79**, 8411.
35 P. Lee and D. Meisel, *J. Phys. Chem.*, 1982, **86**, 3391.
36 J. M. Lerner, R. J. Chambers and G. Passereau, *Proceedings SPIE*, 1981, **268**, 122.
37 M. Moskovits, L. Tay, J. Yang and T. Haslett, *SERS and the single molecule*, Springer-Verlag, Berlin, 2002.
38 C. Galloway, P. G. Etchegoin and E. C. Le Ru, *Phys. Rev. Lett.*, 2009, **103**, 063003.
39 S. Mahajan, R. M. Cole, J. D. Speed, S. H. Pelfrey, A. E. Russell, P. N. Bartlett, S. M. Barnett and J. J. Baumberg, *J. Phys. Chem. C*, 2010, **114**, 7242.
40 T. Itoh, K. Yoshida, V. Biju, Y. Kikkawa, M. Ishikawa and Y. Ozaki, *Phys. Rev. B*, 2007, **76**, 085405.
41 K. D. Shirshendu, B. Davis, D. Ben-Amotz and V. J. Davisson, *Appl. Spectrosc.*, 2008, **62**, 1001.

Supplementary information for "Bi-Analyte Single Molecule SERS with Simultaneous Spatial Resolution"

Determination of the spatial resolution of the CCD

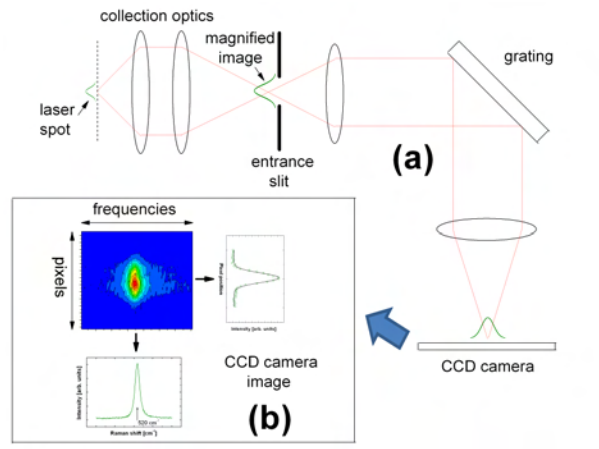

FIG. S1: (a) Schematic representation of the spectrometer. The laser spot on the sample is amplified by a fixed magnification factor of the collecting optics onto the entrance slit of the spectrometer; which in our machine is the same as the confocal pinhole and it is computer controlled. The magnification of the collecting optics in our system for a $\times 100$ objective is $X = 56$. The Raman signal on Si is studied as a function of the pinhole (entrance slit) size, following the protocols developed in the supplementary information of Ref. [1]. The Raman signal in this case is proportional to the area of the spot that is being allowed through at the entrance slit. In (b) we show the result of analyzing the CCD image by projecting (integrating) the signal along the frequency or spatial dimensions. The signal projected on the frequency dimension is the standard Raman spectrum with a width (in pixels) decided by the dispersion of the grating. The signal projected on the spatial dimension, on the other hand, has information on the actual size of the magnified beam on the entrance slit (in the direction parallel to the grooves of the grating). This information is, however, somewhat convoluted by the astigmatic spread of the spectrometer. See the text for further details.

The determination of the spatial resolution on the CCD is not straightforward for a variety of reasons that will be explained in more detail here to complement the information on the main paper. Initially, we characterize the Gaussian beam profile of the laser on the sample. This is a required step to understand the final image produced on the CCD. The characterization of the beam waist of the Gaussian excitation profile on the sample is done by following the protocol developed in full in the supplementary information of Ref. [1] (see also the supplementary information of Ref. [2] for further examples). We summarize here briefly the main points. Essentially, we study the variation of the Raman signal of Si as a function of the confocal pinhole size; which in our machine (Jobin Yvon LabRam UV/Visible) is the same as the entrance slit. In Fig. S1(a) we represent schematically the optical layout. For a $\times 100$ objective used in collection, the laser spot is magnified by a factor of $X = 56$ onto the entrance (confocal) slit of the spectrometer. The latter is square-shaped and can be computer controlled in the range $0-1000\,\mu$m (diagonal size). By studying the variation of the Raman signal as a function of the pinhole size –and fitting the result to an error function (the integral of a Gaussian)– it is possible to measure the beam waist of the laser spot (w_0). The spot itself on the sample can be well represented by a Gaussian intensity profile of the type [1]:

$$I(\rho) = I_0 \exp\left(-\frac{2\rho^2}{w_0^2}\right), \tag{S1}$$

where I_0 is the power density at the centre, and ρ is the radial direction on the focal plane of the sample (measured from the beam center). I_0 [W/m^2] is related to the power P_0 [W] in the beam through the beam waist w_0 [m] via $P_0 = (\pi w_0^2 I_0/2)$ [1]. Note that w_0 is the radial distance at which the intensity of the Gaussian beam has decreased to $\exp(-2) \sim 13\%$ of the intensity at the top. The actual fit to an error function of the experimental data is more complicated in reality, because one normally allows for a small offset (x_0, y_0) in the alignment of the beam; thus resulting in a fit with three independent parameters: x_0, y_0, and w_0 (see Eq. S37 in the supplementary information of Ref. [1]). It is normally a prerequisite that the beam is aligned as perfect as possible with the optical axis of the instrument to perform the slit scan. From there, w_0 can be obtained through the magnification of the collecting optics (X). This method of determining the beam waist of the laser is based on well established knife-edge techniques for beam profiling [3], with the only proviso that it is done here through the Raman signal rather than the intensiy of the laser itself.

An important point is the following: in this initial stage, the Raman signal on the CCD (Fig. S1(b)) is not analyzed in its details at all; the whole signal is integrated with the appropriate binning of the CCD in both the spatial and frequency dimensions, and it only represents a signal *proportional* to the area of the beam being allowed through at the entrance (confocal) slit. The signal on the CCD itself can be deformed or distorted by aberrations or imperfections, but it is still a

valid measure of the total intensity for as long as all the signal is integrated with an appropriate binning of the CCD. Typical values of w_0 obtained with this method are a fraction of the wavelength being used (λ) for diffraction limited spots achieved with high numerical aperture objectives (like $\times$100, NA=0.9). A much more difficult problem is to interpret the exact image on the CCD, which is our next task. This is required if simultaneous spatial and frequency information is sought.

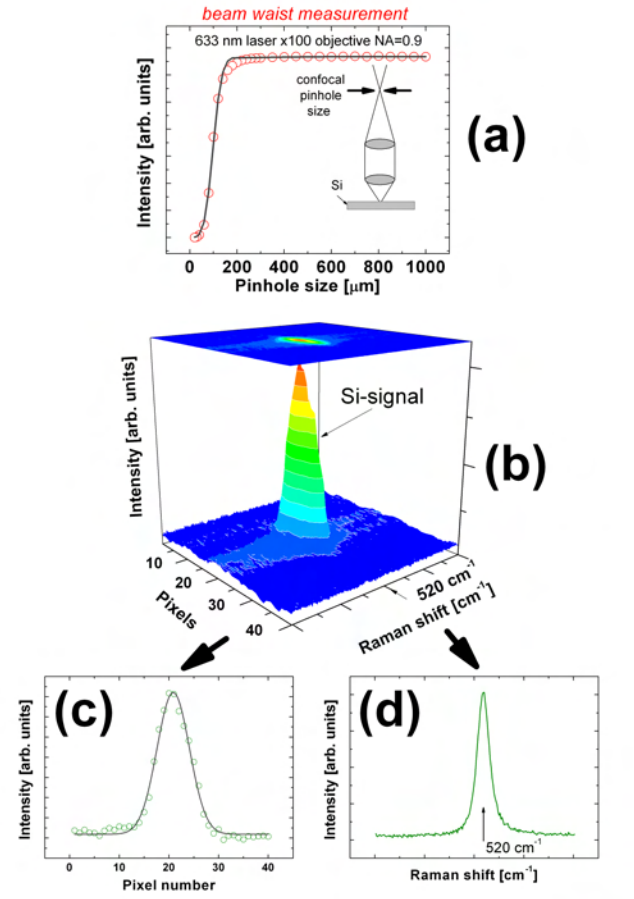

FIG. S2: (a) Beam waist (w_0) characterization using the confocal pinhole dependence [1, 2] of the 520 cm^{-1} Raman mode of Si. From a fit of the the pinhole dependence (red line) we obtain $w_0 = 460$ nm. This implies a magnified beam at the entrance slit with a waist of $Xw_0 = 25.8\,\mu$m, which is imaged after going through the grating onto the CCD as shown in (b). The projected (integrated) signal in the frequency dimension provides the Gaussian spatial profile in (c), while (d) shows the standard Raman signal of Si (at 520 cm^{-1}) projected (integrated) along the spatial dimension axis. From a Gaussian fit to the data in (c) and the determination of w_0 from (a), we could obtain the conversion factor $K = w_0/w_p$ between pixels and real dimensions. The spatial dimension, however, is affected by the presence of astigmatism, as explain further in Figs. S3 and S4.

To analyze the image on the CCD, we start first with the description of the idealized case, and then develop further the interpretation to account for the presence of astigmatism. The idealized situation could be described as follows: Once w_0 is known, it is also known that a magnified version of the Gaussian intensity distribution on the sample exists on the entrance slit (with a magnified beam waist = Xw_0). The spectrometer itself (internally) has a magnification = 1 between the entrance slit and the image on the CCD. The image of the Raman peak on the CCD can now be analyzed in more detail, as shown schematically in Fig. S1(b). The image has basically two dimensions: the spatial one (parallel to the grooves on the grating), and the frequency one (perpendicular to the grooves). In the frequency dimension, the image will spread over a distance (in pixels) which is fixed by the dispersion of the grating. The signal integrated in the spatial direction –for different pixels in the frequency axis– is what is normally measured in the spectrometer as "the Raman peak". On the other hand, the signal integrated in the frequency direction –for different pixels in the spatial dimension– reveals a profile that comes, in principle, from the magnified version of the laser spot on the entrance slit, in the direction parallel to the grooves of the grating. In the spatial direction of the CCD the spectrometer behaves basically as an imaging microscope, subject to the standards constraints of the diffraction limit and image aberrations [4]. This is schematically represented in Fig. S1(b).

However, a *bona fide* estimation of the beam size on the CCD reveals that there is a problem. The Gaussian profile of the spot on the CCD (integrated in the frequency dimension) can be fitted to:

$$I(p) = A \exp\left(-\frac{2(p-p_0)^2}{w_p^2}\right), \qquad \text{(S2)}$$

where A is a constant, p is the pixel number, p_0 is the central pixel, and w_p is the beam waist in pixel units. In principle, w_0 in real (distance) units should correspond to w_p in pixel units under perfect imaging conditions. From here, we could immediately obtain the conversion factor $K = w_0/w_p$ between pixels and real dimensions on the spot.

Figure S2 shows an actual measurement for our system. In Fig. S2(a) we show the beam waist characterization [1, 2] using the entrance (confocal) pinhole (from where we obtain $w_0 = 460$ nm), while Figs. S2(b-d) show the CCD image with its projected (integrated) signals in the spatial and frequency dimensions. From the fit to w_0 in Fig. S2(a) and that to w_p in Fig. S2(c), we could obtain –in principle– the conversion factor $K = w_0/w_p$. However, there is a problem with this value and that can be appreciated from the fact that the

real (physical) pixel size of our CCD is $26\,\mu\text{m} \times 26\,\mu\text{m}$ according to factory specifications. If the original beam on the sample has a waist of $w_0 = 460\,\text{nm}$ (determined by the knife-edge profiling in the previous step) and it is magnified by a factor of $X = 56$ on the entrance slit, then most of the beam should be contained within a radius of $\sim 25\,\mu\text{m}$; i.e. $\sim 1-2$ pixels (perhaps $\sim 3-4$ if a bit of inter-pixel spreading is allowed). But this is not what happens in Fig. S2(b), and the main reason for this is astigmatism [4].

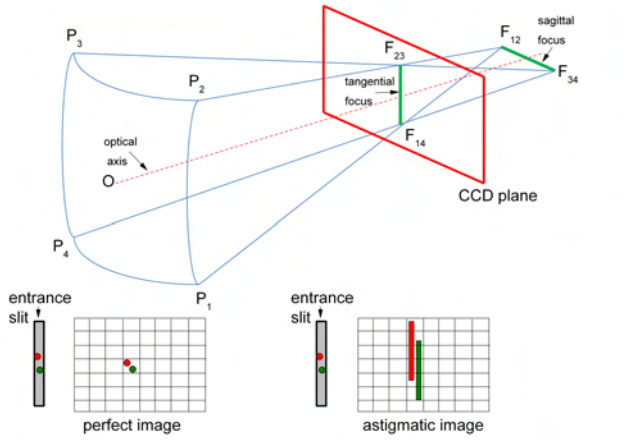

FIG. S3: Astigmatism is produced by the different curvature of the optics in different directions (here exemplified by a simple collecting mirror). The tangential (sagittal) focal plane produces an astigmatism-free image in the horizontal (vertical) direction. In normal spectrometers, the optics is optimized for the CCD plane to be at the tangential focus. In a perfect situation, point-like sources at the entrance slit will be imaged into equivalent points on the CCD plane. However, under the presence of astigmatism, point-like sources are imaged into vertical lines at the tangential focal plane of the CCD. These two examples are shown schematically at the bottom. See Ref. [5] for further details.

Unless one works with special spectrometers with toroidal optics [5] (or aberration-corrected prism spectrometers, like the PARISS spectrometer [5] used in fluorescence) most spectrometers will be optimized to compensate for astigmatism at the tangential focal plane, as depicted in Fig. S3. This is because the horizontal axis is the one containing the spectral information, and we do not want any additional instrumental blurring on that axis (except for the one produced by the natural linewidth of a peak, the dispersion of the grating, the slits setting, and the finite size of the imaged object). The presence of astigmatism in the vertical axis is not much of a problem under normal circumstances, for typically we will be integrating several lines of diodes on the CCD along the vertical direction with an appropriate binning. Therefore, under the normal operating mode of the spectrometer astigmatism is automatically accounted for and is pushed into a dimension where it is not a problem. Nevertheless, it does become a matter of concern if we want to retrieve both spatial as well as spectral information simultaneously.

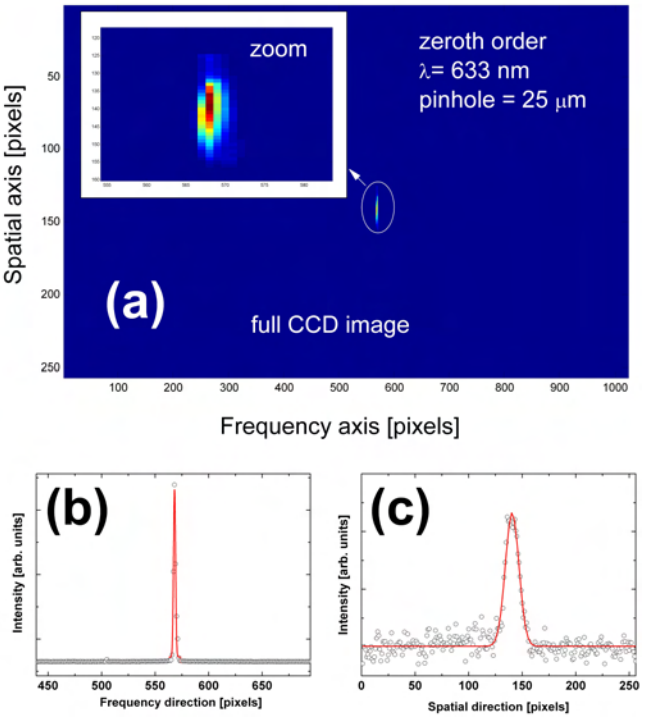

FIG. S4: Experiment to show the presence of astigmatism. The image of the attenuated laser (633 nm) through an entrance slit of $25\,\mu\text{m}$ is taken on the CCD with the grating at zeroth-order (i.e. working as an imaging device). Under ideal conditions, most of the image on the CCD should be contained within $\sim 1-2$ pixels in both horizontal and vertical directions. However, the vertical spread of the image in (a) is ~ 8 times larger in the vertical (spatial) direction than in the horizontal (frequency) one. This can be quantified by looking at the projections of the signal on both axes, as shown in (b) and (c). The CCD is at the tangential plane and the astigmatic spread is more pronounced in the vertical direction.

In order to demonstrate that there is indeed an astigmatic spread in the vertical (spatial) direction, the following experiment was carried out: The laser was carefully aligned to hit the entrance slit in the middle and this was set to a size of $25\,\mu\text{m}$. The grating is set at its zeroth order (reflection) and an image of the entrance slit is obtained. The spectrometer works in this case as an "imaging device" and with an internal magnification =1 we expect most of the image to be concentrated within 1-2 pixels (3-4 with some inter-pixel blurring) in both directions. Fig. S4(a) reveals that the image of the entrance slit is indeed concentrated (mostly) on one central pixel in the horizontal direction, but it is eight times more spread out in the vertical axis. This

can be directly quantified by looking at the (integrated) projections of the signal along both axes, as shown in Figs. S4(b) and (c).

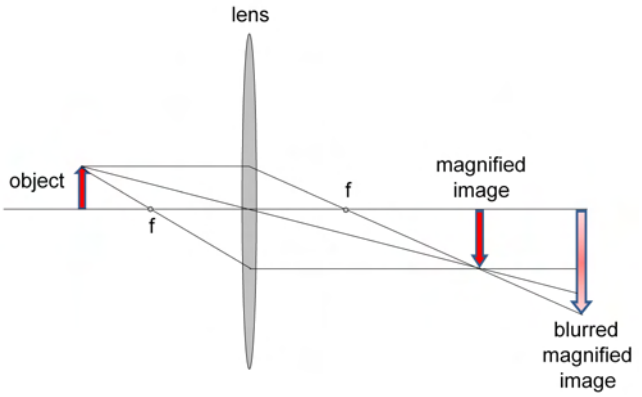

FIG. S5: Magnification with blurring outside the normal focal plane does not result in an increased spatial resolution. We exemplify this here with the example of a simple imaging system consisting of one lens. Each point in the blurred image beyond the image plane has a *point spread function*, exactly like the one that appears through other aberrations (like astigmatism). Even though when the image is magnified and a connection can be made with the original image, it does not result in an increased ability to resolve spatial details. Moreover, single points in the image make contributions to multiple point in the defocused one, thus resulting in the blurring of spatial information.

The result in Fig. S4, however, can still be affected by the finite size of the image on the entrance slit, and this is where it becomes interesting to know what the astigmatic spread would be for an ideal point-like source. But this is, indeed, one of the answers one can get by looking at signals from single molecules. From an experimental point of view, we can claim SM-spectra to be the best possible realization of a point-like source. In fact, this is a possible application of SM-spectroscopy, namely: the experimental realization of point-like emitters to analyze fundamental aspects of the optics of instruments. The width of SM-events in the spatial dimension define the so-called *astigmatic point spread function* (APSF) of the instrument. By looking at different SM-events in the spatial dimension of the CCD in Fig. 3(d) of the main paper we see that the APSF has typical widths in the range of 7-pixels. The illumination profile of the laser (which should have been contained within 1-2 pixels under ideal conditions) is convoluted with the APSF and it obviously dominated by it. Indeed, Fig. 3(d) of the main paper shows that the illumination envelope on a Si sample can accommodate $\sim 1-1.5$ SM-events in the spatial dimension. Therefore, this increase in size by blurring should not be considered as a magnification when we are trying to relate distances on the CCD image plane with distances on the real sample. This is, in fact, the case for any optical image with aberrations (including plain ones, like defocusing, as shown schematically in Fig. S5).

The presence of a "natural spread" from the APSF implies in practice for our case that if peaks happen at exactly the same frequency (horizontal axis) they need to be separated by (at least) 4 pixels to be distinguishable as two separate peaks. This implies a size of $\sim 100\,\mu$m on the CCD (taking the pixel size as $\sim 25\,\mu$m; i.e. $\sim 1.7\,\mu$m on the real sample (after demagnification by a factor of $X = 56$). If the peaks are *not* at the same frequency, as it happens in some mixed events, they can be distinguished in the spatial axis within a single pixel (i.e. $\sim 450\,$nm, in the best of cases). Simultaneous peaks at the same frequency can appear as far apart as $\sim 10-15$ pixels, which represents distances of the order of $\sim 4-5\,\mu$m. In any case, all these estimations give values well above the diffraction limit which is $\sim 380\,$nm for $\lambda = 633\,$nm. Therefore, there is no super-resolution here, or similar claims that have been made for SM-SERS [6]. The only claim here is the experimental fact that we observe SM-events that are spatially resolved, and that those would have been "integrated" and mingled by the CCD binning in the standard implementation of the bi-analyte SERS technique. Here, however, we gain an additional insight into the origin of the signals, including the presence of different molecules at slightly different frequencies (contributing to the inhomogeneous broadening of the peaks [7]), and the existence of Surface-Enhanced Fluorescence (SEF) backgrounds that can be traced back to individual single molecules.

A final question remains though, and this is related to the experimental fact that SM-SERS events can be observed as far apart as $\sim 4-5\,\mu$m. This comes indeed from an additional effect present in our experiments: the perturbation of the beam illumination by the presence of metallic clusters in the sample. It turns out that a beam waist characterization like that in Fig. S2(a) but done on top of colloidal clusters reveals perturbations in the tail of the beam that go all the way to $\sim 400-700\,\mu$m (in confocal slit size). At $\sim 300\,\mu$m slit size, for example, we could easily have $\sim 10-20\%$ of the signal spread on the tail of the beam when it is focused on clusters. This, combined with the huge enhancements of some SERS hot-spots, makes it possible to observe SM-events that are separated as far apart as $\sim 5\,\mu$m on the sample (taking into account the magnification of $X = 56$). In fact, these are the examples that look normally *clearer* in the statistics, for the events are widely seraparated in the spatial dimension and they are easy to identify. It is interesting to note then that the events that show the clearest separation of SM-signals in the spatial

dimension are those in which the illumination comes (mainly) from an "unwanted" effect of spreading the beam by focusing on metallic clusters.

In summary, the spatial dimension of the CCD image contains contributions from the standard magnification of the collecting optics and the natural blurring of astigmatic aberrations. With some natural limitations, signals by single molecules can be spatially resolved and analyzed for their contributions to the overall signal in the bi-analyte method. The combination of spatial and spectral information opens a new dimension into the origin of many effects that are seen in single molecule SERS experiments.

[1] E. C. Le Ru, E. Blackie, M. Meyer, and P. G. Etchegoin, J. Phys. Chem. C **111**, 13794 (2007).

[2] J. E. Bohn, P. G. Etchegoin, E. C. Le Ru, R. Xiang, S. Chiashi, and S. Maruyama, ACS Nano **4**, 3466 (2010).

[3] W. Plass, R. Maestle, K. Wittig, A. Voss, and A. Giesen, Optics Communications **134**, 21 (1997).

[4] M. Born and E. Wolf, *Principles of Optics, 6*$^{\text{th}}$*-edition* (Pergamon Press Ltd., Oxford, 1980).

[5] J. M. Lerner, Cytometry, Part A **69A**, 712 (2006).

[6] S. M. Stranahan and K. A. Willets, Nano Lett. **10**, 3777 (2010).

[7] P. G. Etchegoin and E. C. Le Ru, Anal. Chem. **82**, 2888 (2010).